# Ligand Exchange on Colloidal CdSe Nanocrystals Using Thermally Labile *tert*-Butylthiol for Improved Photocurrent in Nanocrystal Films

David H. Webber and Richard L. Brutchey*

Department of Chemistry and the Center for Energy Nanoscience and Technology, University of Southern California, Los Angeles, California 90089, United States

Ⓢ *Supporting Information*

ABSTRACT: As-prepared CdSe nanocrystals were ligand exchanged using *tert*-butylthiol, which yielded stable CdSe nanocrystal inks in the strong donor solvent tetramethylurea. The efficacy of ligand exchange was probed by thermogravimetric analysis (TGA) and FT-IR spectroscopy. By studying sequential exchanges of tetradecylphosphonic acid and then *tert*-butylthiol, TGA and energy dispersive X-ray spectroscopic evidence clearly demonstrated that the ligand exchange is essentially quantitative. The resulting *tert*-butylthiol-exchanged CdSe nanocrystals undergo facile thermal ligand expulsion (≤200 °C), which was studied by TGA-mass spectrometry. Mild thermal treatment of *tert*-butylthiol-exchanged CdSe nanocrystal films was found to induce loss of quantum confinement (as evidenced by UV−vis spectroscopy) and provided for increased electrochemical photocurrent, electron mobility, and film stability. Pyridine-exchanged CdSe nanocrystals were employed as a control system throughout to demonstrate the beneficial attributes of *tert*-butylthiol exchange; namely, lower organic content, better colloidal stability, improved interparticle coupling, and vastly increased electrochemical photocurrent response upon illumination.
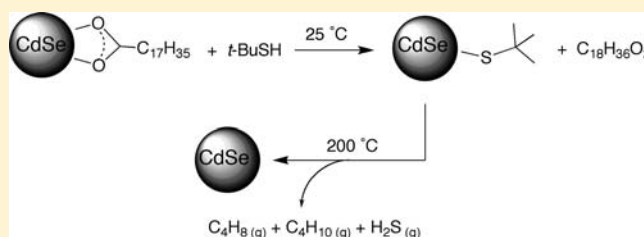
1. INTRODUCTION

Driven by the need to inexpensively fabricate large area photovoltaics, the problem of depositing semiconductor thin films is attracting increased attention. High vacuum techniques such as sputtering, chemical vapor deposition (CVD), and atomic layer deposition (ALD) can achieve high-quality thin films, but low deposition speeds, high cost, limited scalability, and/or high processing temperatures can all be limiting depending on the particular process and material to be deposited.[1] A conceptually attractive alternate route to semiconductor thin films involves preformation of the desired semiconductor in nanocrystal form, followed by solution deposition of a colloidal ink onto the substrate by spray coating,[2a] inkjet printing,[2b,c] spin- or dip-coating.[2d–f]

In addition to their small size that can allow for band gap tuning as a result of quantum confinement effects, semiconductor nanocrystals also have large surface-to-volume ratios. Consequently, the optoelectronic properties of these semiconductor nanocrystals are strongly dependent on their surface chemistry. The ligands that are present during nanocrystal synthesis play a key role in controlling nucleation and growth and also are needed for solvent dispersibility. These native, or legacy, ligands are generally electrically insulating, long-chain aliphatic compounds, such as oleate, stearate, or alkylphosphonates.[3] Such ligands have a disastrous effect on the conductivity and carrier mobility in films due to interparticle insulation; thus, current research is largely focusing on ameliorating this problem since it remains one of the largest barriers to successful ink-based photovoltaics.[3,4]

One approach that can be used to increase carrier mobility is to perform a ligand exchange after the nanocrystals have been deposited as a thin film containing the native ligands.[5] Such an approach can give greatly improved conductivity in the thin film; however, there are several disadvantages inherent to it. The chemicals that are typically used can be toxic and/or caustic (e.g., hydrazine). Second, thick films are difficult to ligand exchange because of (i) diffusion limitations, and (ii) because the volume change that occurs as a result of replacing the native long-chain ligands with small molecules or ions often results in film cracking.[5b] As a result, many iterative cycles of film deposition and ligand exchange can be required to produce good quality films of reasonable thickness. Yet another approach is to remove the native ligands after nanocrystal deposition through heating; however, this can result in disadvantageous coking from incomplete ligand pyrolysis, and high temperatures (∼400 °C) are required to induce loss of quantum confinement and maximize conductivity.[6]

The exchange of insulating ligands for smaller ligands can also be done in the liquid colloidal phase. Among the most commonly used procedures is to exchange the native ligands with pyridine[2d,7] or butylamine,[8] but exchange is generally incomplete with such weak neutral ligands because complete exchange of anionic ligands (charged balanced by an excess of metal cations near the particle surface) is unfavorable.[9] In our own experience with such systems, we have also found a considerable tendency for pyridine- and

butylamine-treated nanocrystals to irreversibly agglomerate on storage. Moreover, the resulting thin films require annealing at high temperatures (>300 °C) for long periods of time to remove the nondisplaced native ligands. As a result, stronger binding small ligands have recently begun to be employed; for example, Talapin and co-workers ligand exchanged CdSe nanocrystals using hydrazinium chalcogenometallates (e.g., $(N_2H_5)_4(Sn_2S_6)$ and $(N_2H_4)_2(N_2H_5)_2In_2Se_4$ complexes).[10] The exchanged particles produced films of greatly improved electron mobility; however, these ligand exchange procedures require the use of hydrazine. Subsequently, Murray and co-workers demonstrated that $NOBF_4$ could be used to effectively ligand exchange a series of nanocrystal types;[11] however, this procedure is limited to oxidation- and acid-stable materials. Thus, there is continuing need to explore new methods of small molecule ligand exchange to help solve some of the limitations of current methods, such as using metal-free inorganic ions or thermally degradable alkyldithiocarbamates.[12]

Herein, we employ CdSe nanocrystals as a model system for an investigation of ligand exchange, replacing the native ligands (NLs; i.e., stearate, alkylphosphonates) with the much smaller *tert*-butylthiol (*t*-BuSH, tBT) ligand. The tBT ligand is commercially available and inexpensive, possesses low toxicity, and can be handled in air. The tBT-exchanged CdSe nanocrystals, or CdSe(tBT), form stable dispersions in strong donor solvents of moderate overall polarity (e.g., tetramethyl-urea, TMU) up to very high concentrations (140 mg mL^{-1}). Cadmium(II) is sufficiently chemically soft, particularly when bonded to selenium, that thiol/thiolate coordination is favorable and exchange proceeds in the desired direction.[13] We have effectively demonstrated removal of the native ligands using thermogravimetric analysis (TGA) and FT-IR spectroscopy, and further shown the efficacy of the exchange by carrying it out on phosphonate-coated CdSe and demonstrating disappearance of phosphorus using energy dispersive X-ray (EDX) spectroscopy. The surface bound ligand cleanly pyrolyzes and decomposes to gaseous byproducts under remarkably mild heating (≤200 °C), resulting in much improved interparticle coupling and loss of quantum confinement, as indicated by UV–vis spectroscopy. Furthermore, we have gained qualitative insights into the ligand pyrolysis mechanism through TGA-mass spectrometry (TGA-MS). The CdSe(tBT) ink can be readily deposited as thin films, which display markedly improved electrochemical photocurrent generation (relative to a pyridine-exchanged CdSe control) after mild heat-treatment.

2. EXPERIMENTAL SECTION

General Considerations. $CdCO_3$ (99.998% metals basis, "Pura-tronic" grade, Alfa Aesar), selenium (200 mesh powder, 99.999% metals basis, Alfa Aesar,), tri-*n*-octylphosphine oxide (TOPO, 98%, Alfa Aesar), sulfur (precipitated, 99.5%, Alfa Aesar), tri-*n*-octylphos-phine (TOP, ≥97%, Strem), tetradecylphosphonic acid (≥97%, Strem), stearic acid (95%, Sigma-Aldrich), 2-methyl-2-propanethiol (*tert*-butylthiol, tBT, 99%, Sigma-Aldrich), aqueous ammonia (28.0–30.0%, "GR ACS" grade, EMD), pyridine (≥99.0%, "GR ACS" grade, EMD), NaOH (99%, "AR ACS" grade, Mallinckrodt), and Na_2S hydrate (>60% Na_2S, Lancaster) were used as received.

Tetramethylurea (TMU, 99%, Alfa Aesar) was distilled at atmospheric pressure under nitrogen before use, discarding ∼5–10% residue in the distillation flask. Distillation was found necessary to remove a sticky yellow evaporation residue present in the as-purchased material.

Synthesis of Native-Ligand CdSe Nanocrystals, CdSe(NL). The synthesis is based on literature methods.[13] In a typical synthesis,

$CdCO_3$ (3.50 g, 20.3 mmol), stearic acid (30.0 g), and tri-*n*-octylphosphine oxide (TOPO, 30.0 g) were stirred at 100 °C under flowing nitrogen (1.5 h), then held at 360 °C under static nitrogen (1 h). With rapid stirring, TOP/TOPSe (selenium (2.30 g, 29.1 mmol) previously dissolved in TOP (30 mL, 67 mmol) under nitrogen) was quickly injected (∼9 s), immediately followed by an injection of octadecene (∼8 s; 30 mL, previously nitrogen-sparged). Exactly 2 min after the start of injection, the flask was removed from the heating bath and the reaction was quenched via cooling in the fume hood draft. When nearing room temperature, 30 mL of nitrogen-sparged toluene was injected to aid the work up.

The product was split between six 45-mL centrifuge tubes and the remaining reaction dregs were collected using 10 mL of toluene. To this was added MeOH (60 mL) and EtOH (66 mL), and the mixture was centrifuged down (6000 rpm, 6 min) and then the supernatant was discarded. To wash the nanocrystals, the solid was redispersed in toluene (120 mL), after which EtOH (150 mL) was added as a flocculant, the mixture was centrifuged (6000 rpm, 1 min), and then the supernatant was discarded. This washing procedure was repeated two additional times, using 120 mL of toluene and 120 mL of EtOH each time. Optionally, the particles were then divided between 4 centrifuge tubes and washed a further five times, using 60–80 mL of toluene and an equal volume of EtOH each time. The final redispersion was done in 60 mL of toluene, followed by centrifugation (6000 rpm, 1 min) to discard the small residue of agglomerates, and then the dispersion was finally passed through a single 450-nm syringe filter to give the final product. The product was stored in the dark at 10 °C.

Concentration Determination. Nanocrystal concentration was done gravimetrically in duplicate by drying a measured volume of solution, weighing the residue, performing TGA, and taking the 600 °C TGA mass as representing pure CdSe. Typical final concentrations were 43–46 mg mL^{-1}, representing a recovered yield of 3.3 g, that is, 85% of the theoretical maximum (after correction for manufacturer's cadmium analysis of the $CdCO_3$ batch used).

Pyridine-Exchange of CdSe Nanocrystals, CdSe(Py). A CdSe-(NL) dispersion in toluene (800 mg CdSe; 18.8 mL) was added to 61 mL of pyridine in a 100-mL round-bottomed flask fitted with a small air-cooled condenser. The system was vigorously nitrogen-purged for ∼10 min, and then introduced into a 90 °C oil bath with slow stirring. The temperature fell to 70 °C and stabilized, and heating was continued for 3 h. After cooling, the dispersion was divided between 12 45-mL centrifuge tubes. These were processed two at a time since after adding antisolvent, a quick workup was found to be important to prevent irreversible agglomeration. Pentane (40–42 mL per tube) was added, the mixture was centrifuged down (6000 rpm, 30 s), and the supernatant was discarded and either pyridine or CdSe-in-pyridine from previous tubes was immediately added in order to disperse the solid. (Note: It is essential to add the redispersion mixture as rapidly as possible to avoid the solid drying out.) The total volume of pyridine used for redispersion was 6 mL. The dispersion was centrifuged (4000 rpm, 2 min) and carefully decanted from the small precipitate of agglomerates in order to give the final product. Concentration determination typically gave ∼77 mg mL^{-1} of CdSe. The product was stored in the dark at 10 °C.

***tert*-Butylthiol-Exchange of CdSe Nanocrystals, CdSe(tBT).**

(1) Particle recovery: CdSe(NL) in 12-mL of toluene (42.5 mg mL^{-1} of CdSe; 510 mg total CdSe) was placed in a 45-mL centrifuge tube, an equal volume of TMU and tBT (2 mL) were added, and finally a sufficient amount of MeOH was added to flocculate before centrifugation (6000 rpm, 1 min). The colorless supernatant was discarded.

(2) Ammonia-assisted ligand exchange (repeated four times): To the nanocrystals were added TMU (5 mL), tBT (1 mL), and concentrated aqueous NH_3 (0.2 mL for the first wash and 0.1 mL thereafter). This mixture was rapidly stirred to produce a clear colloid. To this mixture was added MeOH (20 mL) and pentane (not required for the first wash, ∼15–25 mL required

in the subsequent washes for satisfactory flocculation), followed by centrifugation (6000 rpm, 1 min), and discarding of the supernatant. Care was taken to not allow the particles to dry out at any stage, as drying caused irreversible agglomeration. Note: As an alternative to using MeOH and pentane to induce flocculation, MeOH and additional concentrated aqueous NH_3 (~1 mL) was also highly effective, although may possibly be too aggressive if done repeatedly.

(3) Removal of excess NH_3 (repeated twice): To the nanocrystals were added TMU (5 mL first time and 4 mL the second) and tBT (1 mL). The mixture was rapidly stirred to very easily form a clear colloid. To this mixture was added MeOH (10 mL) and pentane (25 mL first time and 20 mL the second), followed by centrifugation (6000 rpm, 1 min), and discarding of the supernatant.

(4) Removal of excess MeOH to allow for final redispersion in a minimum of TMU: To the nanocrystals were added TMU (4 mL) and tBT (1 mL). The mixture was rapidly stirred before pentane (30 mL) was used to flocculate the particles, which were then centrifuged (6000 rpm, 1 min) and the supernatant discarded.

(5) Final redispersion: TMU (3 mL) was added to the nanocrystals. The mixture was stirred very rapidly before bubbling nitrogen through the liquid for ~1 min to evaporate residual pentane. At this point, tBT (0.2 mL, antioxidant) was added and the mixture was centrifuged (6000 rpm, 1 min) before decanting off the supernatant from the very tiny mass of precipitated agglomerates. The dispersion was passed through one 450-nm syringe filter before adding 0.2 mL of tBT to form a final dispersion.

The final dispersion was stored cold in the dark for extended periods (many weeks) with no agglomeration or precipitation. (TMU has a relatively high freezing point, but the tBT was sufficient to keep the mixture liquid during cold storage.) The quality of the product was sufficiently high to allow for spin coating without requiring any further filtration steps. Concentration determination typically gave 140 mg mL^{-1} CdSe. Recovered yield of CdSe was 95%.

Tetradecylphosphonic Acid-Exchange of CdSe Nanocrystals, CdSe(TDPA). The required quantity of TDPA was estimated by assuming the TGA mass loss for CdSe(NL) corresponded to a stearate monolayer, and further assuming that stearate occupied two surface sites and phosphonate occupied three (see discussion in Supporting Information). A 3−4% excess was used, based on the above calculation. Typically, a CdSe(NL) dispersion in toluene (10 mL, 425 mg CdSe) was mixed with a premade solution of TDPA (89.6 mg, 0.322 mmol) in *n*-butanol (6 mL) in a 45-mL centrifuge tube. The dispersion was allowed to stand in the dark 1.7 h, and was then flocculated with MeOH (35 mL), centrifuged down (6000 rpm, 6 min), and the supernatant was discarded. The solid was washed by redispersing in 5 mL of toluene, flocculating with 40 mL of MeOH, centrifuging down (6000 rpm, 6 min), and discarding the supernatant. To ensure rigorous elimination of unbound TDPA, the product was washed five more times. Final redispersion was in 8 mL of toluene. To test for agglomeration, the final product was centrifuged (6000 rpm, 1 min) and no solid was deposited, indicating minimal or no agglomeration. Concentration determination typically indicated 49.5 mg mL^{-1} CdSe.

Film Deposition and Characterization Details. Full details are given in the Supporting Information.

3. RESULTS AND DISCUSSION

3.1. Nanocrystal Synthesis and Characterization. The CdSe nanocrystals were prepared using a modified literature procedure in the presence of stearic acid and as-received TOPO,[13] which is known to contain phosphonic acid impurities.[14] The as-prepared CdSe(NL) was washed either three or eight times, using toluene dispersant and ethanol flocculant, and finally redispersed in toluene. The resulting CdSe(NL) nanocrystals were readily dispersible in a series of low polarity solvents (e.g., toluene, chloroform) as a result of

their aliphatic ligand shell. Thermogravimetric analysis indicated the extra five washes removed only a minor proportion of the native ligands (see Supporting Information, Figure S1), and the colloidal stability was not affected. UV−vis spectra of the CdSe(NL) nanocrystals dispersed in toluene showed a clear first exciton peak at 590.8 nm and a partly resolved second exciton absorption with a point of inflection at 481.0 nm (Figure 1). UV−vis spectra were also obtained in
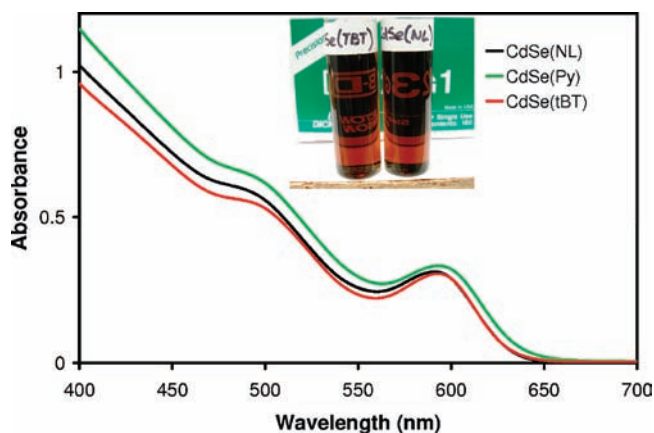
Figure 1. UV−vis spectra of CdSe(NL), CdSe(Py), and CdSe(tBT) nanocrystal dispersions in toluene, pyridine, and TMU, respectively. Photographs of the CdSe(NL) and CdSe(tBT) dispersions in toluene and TMU, respectively, are shown as inset.

$CHCl_3$ to allow sizing by the empirical equation of Jasieniak et al.; the first exciton peak was observed at 590.0 nm corresponding to ~4.3 nm diameter CdSe nanocrystals.[15] A photoluminescence spectrum was obtained using an excitation wavelength of 500 nm; it displayed a clear near-band edge emission at $\lambda_{max} =$ 597 nm (see Supporting Information, Figure S2). Transmission electron microscopy (TEM) analysis of the resulting CdSe-(NL) nanocrystals showed nonagglomerated, roughly spherical particles that were 4.6 ± 0.6 nm in diameter (see Supporting Information, Figure S3). Powder X-ray diffraction (XRD) analysis indicated that the CdSe nanocrystals were in the wurtzite phase with significant Scherrer line broadening, consistent with their small size (see Supporting Information, Figure S4).

3.2. Ligand-Exchange and Characterization. A portion of the CdSe(NL) nanocrystals were ligand exchanged with tBT, as described in the Experimental Section. In brief, the nanocrystals were repeatedly dispersed in TMU and tBT (with ammonia being added in the early steps), flocculated with methanol/pentane, and separated from the supernatant containing the displaced native ligands, with final redispersion in TMU plus a small proportion of tBT as an antioxidant. It should be noted that the ligand exchange can be optionally conducted without ammonia (see Supporting Information), but may not be fully effective in the presence of strongly binding native ligands, such as adventitious phosphonate (*vide infra*). Tetramethylurea was found to be a superlative dispersion medium for the ligand exchange, likely because it is a strong electron-pair donor allowing for additional passivation of the nanocrystal surfaces but with low enough overall polarity to allow for alkane miscibility. Thus, TMU does not flocculate the initial long chain-stabilized nanocrystals and is also compatible with the thiol-coated surfaces of the product. The dispersibility of CdSe(tBT) was markedly superior in TMU than in the slightly weaker donor and higher overall-polarity solvent dimethylacetamide (DMAc).

Tetramethylurea is a strong electron-pair donor solvent (donor number, DN = 29.6) comparable to amide solvents such as DMAc (DN = 27.8).[16a] It also possesses a dipole moment only slightly lower than typical amide solvents (3.47 D vs 3.72 D for DMAc), but with a bulk polarity that is substantially lower than DMAc, as assessed by relative permittivity (23.60 vs 37.78, respectively), or by miscibility number (15 vs 13, respectively).[16] Unlike DMAc, TMU is miscible with all except the longest chain alkanes (e.g., it is miscible with octane but only partly miscible with tetradecane), making it compatible with the tBT ligated surfaces, but still able to stabilize local charges or vacant coordination sites through its strong local dipole and pair donation. The colloidal stability of CdSe(tBT) was excellent in TMU despite the shortness of the tBT ligand, with colloidal suspensions (up to 140 mg mL^{-1}) remaining stable for weeks when stored cold in the dark. This level of stability is unusual for nanocrystals capped with such a short alkanethiol ligand, and the lack of colloidal stability of tBT-capped nanocrystals in more conventional solvents probably accounts for the rarity of this ligand in the nanocrystal literature. The tBT ligand has been employed in the formation of Au nanocrystals, but the crude product agglomerated with time, and was not stable to purification.[17]

As a control, a further portion of CdSe(NL) nanocrystals was subjected to a conventional pyridine (Py) exchange, with pyridine as the final redispersion medium. UV–vis spectra of CdSe(tBT) and CdSe(Py) were taken in TMU and pyridine, respectively (Figure 1). There was little change in the spectral features from CdSe(NL) in toluene, save for slight shifts in the position of the exciton peak (λ_{max} = 590.8, 592.8, and 593.2 nm for CdSe(NL), CdSe(tBT), and CdSe(Py), respectively), which suggests the size, shape, and size distribution of the CdSe nanocrystals are unaffected by ligand exchange. The observed shifts are minor and likely result from differences in the polarity and polarizability of the three solvents.[18]

Analysis of TEM images of the nanocrystals provided further evidence of the integrity of the nanocrystals after ligand exchange, with no significant size or morphological changes being apparent (see Supporting Information, Figures S5, S6a−c). Based on the nanocrystal size and surface ligand coverage derived from TGA data, ligand shell thicknesses were approximated using a simple core–shell volume model (see Supporting Information for full details). The CdSe(NL) nanocrystals were estimated to possess a ligand shell thickness of ∼0.9 nm, which is only slightly larger than half of ∼1.5 nm closest approach distance of analogous oleate-passivated nanocrystals in a close-packed solid.[5c] The CdSe(tBT) nanocrystals were estimated to possess a ligand shell thickness of 0.3 nm; however, it should be noted that many adjacent CdSe(tBT) nanocrystals were observed by TEM to have virtually no interparticle spacing (see Supporting Information, Figure S6c), unlike for CdSe(NL) where there is always visible separation as a result of the long-chain native ligands.

3.3. Thermal Analysis. It was found that TGA analysis (ambient to 650 °C, 10 °C min^{-1}, under nitrogen flow) of samples thoroughly dried at 100 °C provided a striking demonstration of the benefits of tBT ligand exchange (Figure 2). Taking the mass at 600 °C as approximating pure CdSe, it was found that CdSe(NL) nanocrystals typically contained 24% organic matter after three toluene/ethanol washes, and 22% after five additional washes, confirming that the remaining surface material was strongly bound. Pyridine exchange reduced the organic content to around 19%, but tBT treatment resulted in only ∼5−7% organics. Moreover, the majority of the thermolytic mass loss for the CdSe(tBT) was concentrated in a
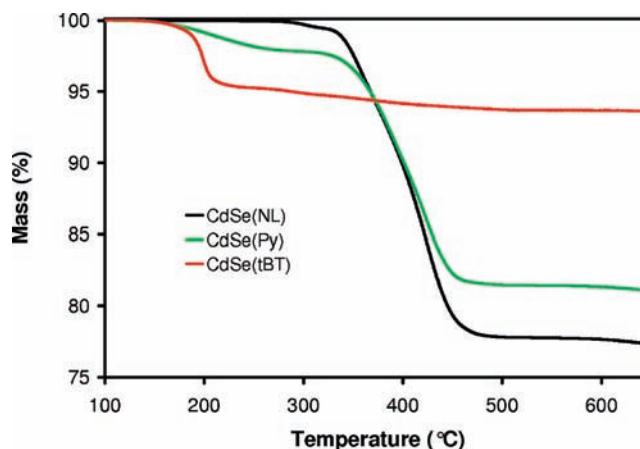

Figure 2. TGA data for CdSe(NL), CdSe(Py), and CdSe(tBT) at a constant heating rate of 10 °C min^{-1} under a flowing nitrogen atmosphere. The samples were dried to constant mass at 100 °C before analysis (∼2 h).

low temperature decomposition step, with up to 89% of the total mass loss occurring below 230 °C, whereas the vast proportion of ligand loss for CdSe(NL) and CdSe(Py) occurred in the range ∼330−470 °C. The particularly small TGA mass loss of CdSe(tBT) indicated a high degree of ligand replacement, explicable on the grounds that neutral native ligands (e.g., TOPO and stearic acid) can be displaced by thiol, but that stronger-bonding anionic ligands (e.g., stearate, adventitious phosphonate) can also be replaced by thiolate via a proton exchange mechanism.[9b] The small mass loss displayed by CdSe(tBT) at >230 °C is likely a result of loss of strongly bound HS$^-$ and S^{2-} remaining after tBT pyrolysis (*vide infra*).

On the basis of the known lability of neutral ligands during washing,[19] the majority of the native ligands is likely stearate on the purified nanocrystals. From a calculated surface area of 240 m^2 g^{-1} (based on a 4.3 nm diameter and 5.81 g cm^{-1} bulk density) and a TGA mass loss of 22% at 600 °C, a surface coverage of 2.5 stearate nm^{-2} can be approximated, which is consistent with literature precedent for related ligands.[20] Similarly, a mass loss of 7% at 600 °C for CdSe(tBT) translates to a surface coverage of 2.2 ligands nm^{-2}, suggesting less dense surface coverage for the sterically demanding tBT ligand.

To probe the utility of low temperature heat treatment for the expulsion of tBT ligands, isothermal TGA experiments were conducted by holding the sample at 200 °C for 2 h before ramping to 650 °C at 10 °C min^{-1} (see Supporting Information, Figure S7). By the end of the isothermal soak, the mass loss as a percentage of the total loss up to 600 °C was 75% for CdSe(tBT), 10% for CdSe(Py), and a miniscule 0.05% for CdSe(NL). The results confirm the utility of tBT as a thermally labile nanocrystal capping ligand, and imply that a 200 °C heat-treatment of CdSe(tBT) films should result in the expulsion of most interparticle insulating matter within a few minutes. The easy expulsion of tBT is in accord with the easy thermolysis of *tert*-butylthiolate complexes, likely a result of the relative stability of *tert*-butyl radical intermediates. The facile thermolysis of *tert*-butylthiolate complexes has been previously demonstrated in (TOP)$_2$CuIn(S^{t}Bu)$_2$, which decomposed at 170 °C (vs 200 °C for the *n*-propylthiolate analog),[21a] and Ca(S^{t}Bu)$_2$, which also decomposed at 170 °C (vs 315 °C for the 1-adamantanethiolate analog).[21b]

TGA-mass spectrometry (TGA-MS) was used to better understand the facile pyrolysis of surface-bound tBT ligands on CdSe (see Supporting Information, Figures S8a–f, Table S1). During the ~200 °C mass loss event, isobutene, isobutane (via t-Bu$^+$), and H_2S were observed as the major volatile products, as shown in Figure 3. The major products are likely accounted
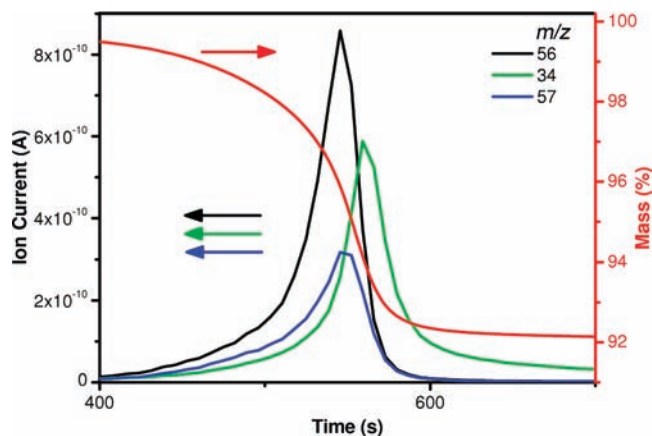

Figure 3. TGA-MS data demonstrating how peak current of the m/z = 34 (H_2S) species is shifted to a distinctly higher temperature and time relative to the m/z = 56 and 57 (isobutene and t-Bu$^+$, respectively) peaks. Release of the m/z = 34 species also continues at much higher temperatures than for the other two species. TGA was performed at 20 °C min^{-1} under argon.

for by simple homolytic bond scission and H-transfer steps, releasing isobutene and isobutane and leaving sulfur and sulfhydryl groups on the surface (see Supporting Information, Schemes S1a–b). Surface sulfhydryl groups may be the source of the observed H_2S, and could account for the observed time and temperature lag between peak isobutane and isobutene evolution and the peak H_2S outflow (Figure 3). Additionally, surface sulfhydryls might also account for the distinct H_2S production up to appreciable temperatures (>350 °C; see Supporting Information, Figure S8c). Only a very small tBT signal was observed, which likely indicates that most tBT was chemisorbed as thiolate rather than in the nondeprotonated thiol form. This is reasonable in view of the published evidence for the much stronger surface binding of thiolate versus thiol on CdSe,[22] and the known propensity of the native ligands (carboxylate and adventitious phosphonate) to bond as anions to surface-excess Cd(II).[9b,23] The products of surface-bound CdSe(tBT) decomposition seem appreciably different from those known to be produced by the >250 °C pyrolysis of Zn(S^{t}Bu)$_2$, which gives equimolar amounts of tBT, H_2C=C(CH$_3$)$_2$, and ZnS,[24] and from the >170 °C pyrolysis of Ca(S^{t}Bu)$_2$, which gave a 45:53 mixture of H_2C=C(CH$_3$)$_2$ and tBT, plus traces of isobutane, ^{t}Bu$_2$S$_2$, and ^{t}Bu$_2$S.[21b] Of sulfur remaining on the surface, it is likely that some was charge balanced by surface-excess Cd(II), and thus present as essentially irremovable CdS; however, there appears to have been an excess of sulfur that was evolved as S_2 and observed as a small signal during the rapid mass loss phase and reappearing again at high temperatures (see Supporting Information, Figure S8f). It should be noted that TMU or its decomposition products were not observed between m/z = 16 to 120, suggesting that it was completely expelled during the drying stage of TGA-MS sample preparation (~85 °C under flowing

nitrogen, 1.5 h) and therefore is not a strongly binding surface ligand.

The TGA data are strikingly supported by FT-IR analysis of the CdSe nanocrystals. The organic content on the CdSe nanocrystals was probed by semiquantitative FT-IR analysis using an internal standard (Figure 4). The nanocrystal samples
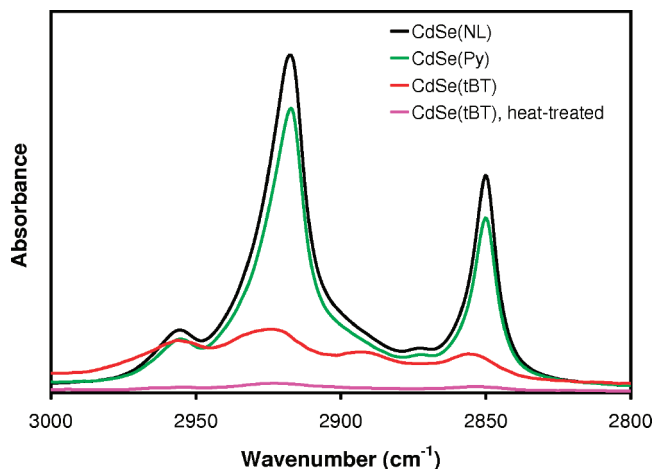
Figure 4. ν(C–H) stretching region in the FT-IR spectrum of CdSe nanocrystals taken in a KBr matrix. The thermally treated CdSe(tBT) was heated to 200 °C. The spectra were normalized to the 2089 cm^{-1} ν(C≡N) stretching peak of a measured Fe$_4$[Fe(CN)$_6$]$_3$ internal standard (not shown).

were either dried at 80–90 °C or heated to 200 °C before analysis. As expected, the results showed absorption in the 3000–2800 cm^{-1} ν(C–H) stretching region reducing in the order, CdSe(NL) > CdSe(Py) ≫ CdSe(tBT) ≫ 200 °C heat treated-CdSe(tBT). The native ligand and pyridine-exchanged CdSe did not show significant changes by FT-IR spectroscopy before and after heat treatment at 200 °C (see Supporting Information, Figure S9), indicating minimal ligand desorption or pyrolysis.

3.4. Efficacy of tBT Ligand Exchange. A tBT-ligand exchange employing a pentane flocculant can be utilized without aqueous ammonia. Under such conditions, ligand exchange on CdSe(NL) was excellent, but TGA often showed a small residuum lost at ~400 °C which was attributed to adventitious phosphonate from the TOP and TOPO starting reagents.[14] To probe this, the CdSe nanocrystals were treated with tetradecylphosphonic acid (TDPA). When the non-ammonia-assisted tBT ligand exchange was applied to CdSe-(TDPA), incomplete removal of phosphonate was observed by TGA (i.e., only ~56% of the phosphonate ligands were lost; see Supporting Information, Figure S10).

Alivisatos et al. found that 2-methoxyethanethiol and 2,5,8,11-tetraoxatridecane-13-thiol would minimally displace octadecylphosphonic acid (ODPA) from CdSe nanocrystals, unless triethylamine were added, whereupon exchange became facile.[9b] Phosphonic acid ligands are known to bond in a deprotonated form (probably monodeprotonated) to a surface-excess of Cd(II) in CdSe nanocrystals.[20] Protonation of surface phosphonate by thiol is highly unfavorable because of the difference in acidities (pK_{a1} = ~2.6 and pK_{a2} = ~8 for n-alkylphosphonic acids; pK_a = ~11.1 for tBT),[25] but in the presence of an amine, the thiol can be deprotonated during the exchange and the phosphonate removed as an ammonium

phosphonate salt.[9b] In light of this, the ligand exchange procedure was modified to incorporate aqueous ammonia. It was found that TDPA had poor solubility in hydrocarbons, likely due to its propensity for hydrogen bonding, so a polar MeOH-based flocculant system was substituted for pure pentane. By TGA, ~44% of the phosphonate ligands remained after ligand exchange with tBT without ammonia, while replacement of phosphonate was essentially quantitative using an ammonia-assisted tBT ligand exchange (see Supporting Information, Figure S10). EDX spectroscopy corroborated the quantitative ligand exchange by showing a total loss of phosphorus from the sample (see Supporting Information, Figure S11). In contrast, TGA demonstrated that pyridine-exchange of CdSe(TDPA) was totally ineffectual, and EDX data showed no loss of phosphorus. Application of the ammonia-assisted tBT ligand exchange to CdSe(NL) invariably resulted in ~100% loss of the native ligands, as evidenced by TGA. Given the known strong binding of phosphonate, the success of the ammonia-assisted tBT ligand exchange on CdSe(TDPA) indicates that the procedure should also be effective at displacing intentional or adventitious native ligands on a variety of CdSe nanomaterials.

3.5. Film Formation and Interparticle Coupling. Approximately 70-nm thick CdSe(tBT) nanocrystal films were examined by scanning electron microscopy (SEM) before and after heat treatment to 200 °C (see Supporting Information, Figure S12). The as-prepared CdSe(tBT) showed relatively continuous films with short microstructural cracks that arose from drying of the concentrated nanocrystal suspension during spin coating. Interestingly, the degree of microstructural cracking does not qualitatively change much upon heat treatment to 200 °C, which suggests that the ligand pyrolysis and decomposition does not exacerbate film cracking due to volume contraction.

The CdSe(NL), CdSe(Py), and CdSe(tBT) nanocrystals were all easily spin coated from their respective solvents to give good quality films. Relatively thick films were spun on glass for UV−vis analysis before and after heat treatment at 200 °C under nitrogen. The as-spun films all showed a clear first exciton peak (λ_{max} = 595.0 nm), the wavelength for all three being essentially identical to within experimental error (Figure 5).
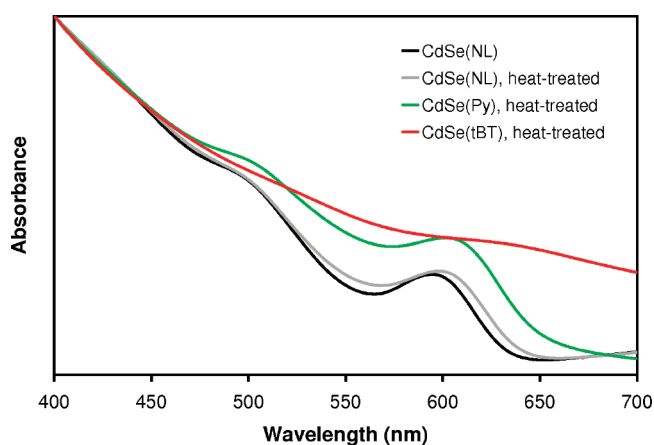
Figure 5. UV−vis spectra of spin-cast films of CdSe nanocrystals, normalized to give equal optical density at 400 nm. Before heat treatment at 200 °C, the CdSe(Py) and CdSe(tBT) films gave essentially identical spectra to CdSe(NL), and have thus been omitted for clarity. The sloping baseline shown by CdSe(NL) beyond 650 nm is likely due to optical interference in the fairly thick film.

After heat treatment to 200 °C, moderate changes were observed in the position of the first exciton peak for CdSe(NL) and CdSe(Py) (λ_{max} = 598 and 601 nm, respectively), whereas the exciton peak for CdSe(tBT) essentially disappeared, leaving only a shallow bathochromically shifted point of inflection at 611.0 nm. The obvious inference is that mild heating to 200 °C is sufficient to drastically increase interparticle electronic coupling in CdSe(tBT) nanocrystal films, but not in CdSe(NL) or CdSe(Py) nanocrystal films, as would be expected from the FT-IR and isothermal TGA data. Analysis of the (100), (002) and (101) Bragg reflections of the CdSe(tBT) film by XRD before and after heat treatment did not show any appreciable peak sharpening, suggesting that gross nanocrystal sintering and grain growth is negligible at 200 °C (see Supporting Information, Figure S13).

3.6. Photocurrent Measurements. Photocurrent measurements on semiconductor nanocrystal films are an effective and convenient method of ascertaining the potential of materials for various photoelectronic applications.[26] Thin films of CdSe(tBT) and CdSe(Py) were deposited by spin-coating on ITO-coated glass substrates to give the same optical density at 472 nm (see Supporting Information, Figure S14), and briefly heat treated at 200 °C under nitrogen. Photocurrent measurements were performed using a three-electrode setup, using Pt counter and pseudoreference electrodes, with two 472 nm LEDs for illumination and an aqueous Na_2S electrolyte (0.2 M).[27] The potential of the Pt reference was measured before and after experiments against an Ag/AgCl reference; corrected to the NHE scale it was found to be −0.55 V. The observed difference in behavior between the CdSe(tBT) and CdSe(Py) films were striking; that is, CdSe(tBT) displayed classic n-type behavior, with repeatable, high anodic photocurrent densities under illumination (ca. −75 μA cm^{-2} at 0 mV relative to Pt pseudoreference), indicative of surface photooxidation of S^{2-} to S_2^{2-} (Figure 6). As
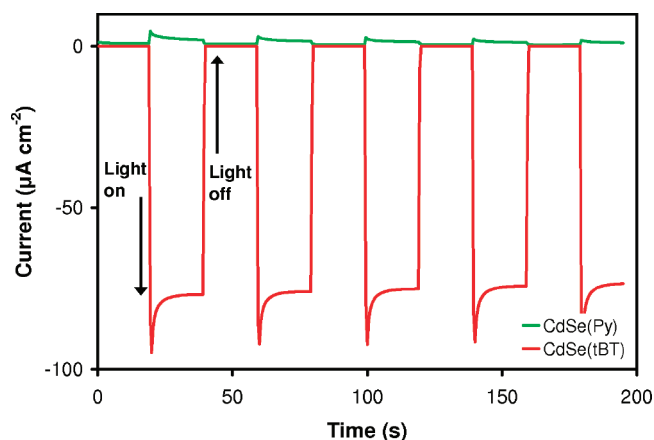
Figure 6. Photocurrent response for 200 °C heat-treated CdSe(Py) and CdSe(tBT) films, at a potential of 0 V relative to a Pt pseudoreference electrode (0 V on this scale = −0.55 V relative to NHE). The ~472 nm (nonmonochromatic) illumination on and off periods are 20 s.

expected from literature precedent, the photocurrent densities increased with increasingly positive potential (Figure 7).[28] Contrarily, the CdSe(Py) displayed very small photocurrents (<2 μA cm^{-2} at 0 mV relative to Pt pseudoreference; see Supporting Information, Figure S15). The CdSe(Py) films generally showed ambipolar behavior, which may be caused by the presence of surface ligands and oxidizing or reducing agents in nanocrystal solids.[5c] The presence of a mixed coordination sphere
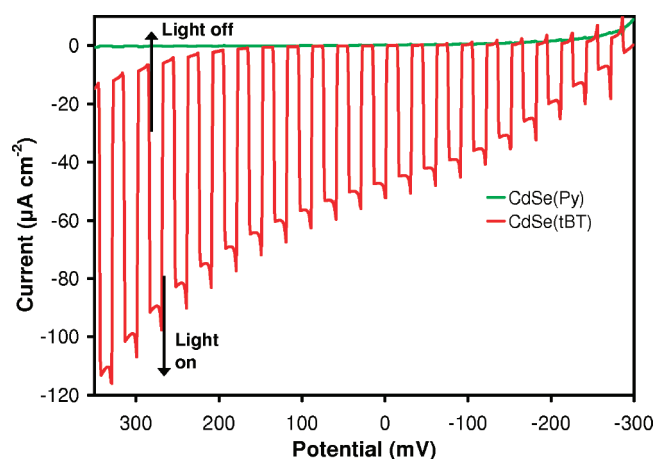
Figure 7. Photocurrent response for 200 °C heat-treated CdSe(Py) and CdSe(tBT) films during a potential scan from −300 to +350 mV (at 3 mV s^{-1}), relative to a Pt pseudoreference electrode (0 V on this scale = −0.55 V relative to NHE). The ~472 nm (non-monochromatic) illumination on and off periods are 5 s.

of pyridine, stearate, and incoming S^{2-} (from the redox mediator) on the CdSe(Py) nanocrystal films may account for this effect.

The CdSe(tBT) films gave a photocurrent up to 70-fold higher than the CdSe(Py) films. Moreover, the CdSe(tBT) films stood up well to the electrolyte under reasonable potentials, but the CdSe(Py) films invariably broke down with time, bleaching in color and detaching if the sample was mechanically agitated (see Supporting Information, Figures S16). It is likely that the improved photoelectrochemical response and improved robustness of the CdSe(tBT) is a function of "bare" particle surfaces and strong interparticle interaction, giving higher photocurrent and stronger film adhesion. In contrast, the high organic loading that remains in the CdSe(Py) nanocrystal film is electrically insulating, and ingress of electrolyte swells the film and damages it. The general conclusions of the electrochemical photocurrent measurements were validated by solid-state field effect transistor (FET) measurements on CdSe(Py) and CdSe(tBT) nanocrystal films. The CdSe-(tBT) nanocrystal films displayed clear n-type behavior with average electron mobilities of $\mu_e = 1.3 \times 10^{-4}$ cm^2 V^{-1} s^{-1}, while the CdSe(Py) nanocrystal films gave much lower currents and displayed marginal n-type behavior with $\mu_e \approx 8 \times 10^{-6}$ cm^2 V^{-1} s^{-1} (see Supporting Information, Figures S17,18).

4. CONCLUSION

In summary, we have developed an easy ligand exchange procedure for CdSe nanocrystals, replacing long-chain native ligands (including strongly bound phosphonate species) with tBT, an inexpensive and readily available ligand. Unlike some literature systems, ligand exchange with tBT does not require non-commercially available reagents, inert atmosphere, or hazardous hydrazine, and operates on the hundreds-of-milligram scale with potentially easy scalability to multigram amounts. The colloidally stable CdSe(tBT) nanocrystals possess low organic content, and quickly lose organics at 200 °C to give an in-organic semiconductor film that exhibits excellent electro-chemical photocurrent as compared to the CdSe(Py) control system. We anticipate that this procedure can be extended to other technologically important semiconductor nanocrystals that have an affinity for thiolate ligands; notably, the chalco-genides of lead, cadmium, tin, silver and copper, in addition to CIGS(e) and CZTS(e) systems.

■ ASSOCIATED CONTENT

ⓢ Supporting Information

Details of ligand exchange and film deposition and character-ization; notes on native ligand identity, size, and coverage; supplemental PL, TEM, FT-IR, UV−vis, XRD, EDX, TGA, TGA-MS, electrochemical and FET data; speculative pyrolysis mechanism. This material is available free of charge via the Internet at http://pubs.acs.org.

■ AUTHOR INFORMATION

Corresponding Author
brutchey@usc.edu

■ ACKNOWLEDGMENTS

■ REFERENCES

(1) Gao, Y.; Koumoto, K. *Cryst. Growth Des.* **2005**, *5*, 1983.
(2) (a) Akhavan, V. A.; Goodfellow, B. W.; Panthani, M. G.; Reid, D. K.; Hellebusch, D. J.; Adachi, T.; Korgel, B. A. *Energy Environ. Sci.* **2010**, *3*, 1600. (b) Haverinen, H. M; Myllyla, R. A.; Jabbour, G. E. *Appl. Phys. Lett.* **2009**, *94*, 073108. (c) Singh, M.; Haverinen, H. M.; Dhagat, P.; Jabbour, G. E. *Adv. Mater.* **2010**, *22*, 673. (d) Gur, I.; Fromer, N. A.; Geier, M. L.; Alivisatos, A. P. *Science* **2005**, *310*, 462. (e) Wu, Y.; Wadia, C.; Ma, W.; Sadtler, B.; Alivisatos, A. P. *Nano Lett.* **2008**, *8*, 2551. (f) Luther, J. M.; Law, M.; Beard, M. C.; Song, Q.; Reese, M. O.; Ellingson, R. J.; Nozik, A. J. *Nano Lett.* **2008**, *8*, 3488.
(3) Talapin, D. V.; Lee, J.-S.; Kovalenko, M. V.; Shevchenko, E. V. *Chem. Rev.* **2010**, *110*, 389.
(4) (a) Habas, S. E.; Platt, H. A. S.; van Hest, M. F. A. M; Ginley, D. S. *Chem. Rev.* **2010**, *110*, 6571. (b) Tang, J.; Sargent, E. H. *Adv. Mater.* **2011**, *23*, 12. (c) Sargent, E. H. *Adv. Mater.* **2008**, *20*, 3958.
(5) (a) Zarghami, M. H.; Liu, Y.; Gibbs, M.; Gebremichael, E.; Webster, C.; Law, M. *ACS Nano* **2010**, *4*, 2475. (b) Luther, J. M.; Law, M.; Song, Q.; Perkins, C. L.; Beard, M. C.; Nozik, A. J. *ACS Nano* **2008**, *2*, 271. (c) Talapin, D.; Murray, C. B. *Science* **2005**, *310*, 86.
(6) Drndic, M.; Jarosz, M. V.; Morgan, N. Y.; Kastner, M. A.; Bawendi, M. G. *J. Appl. Phys.* **2002**, *92*, 7498.
(7) Murray, C. B.; Norris, D. J.; Bawendi, M. G. *J. Am. Chem. Soc.* **1993**, *115*, 8706.
(8) (a) Porter, V. J.; Geyer, S.; Halpert, J. E.; Kastner, M. A.; Bawendi, M. G. *J. Phys. Chem. C* **2008**, *112*, 2308. (b) Johnston, K. W.; Pattantyus-Abraham, A. G.; Clifford, J. P.; Myrskog, S. H.; MacNeil, D. D.; Levina, L.; Sargent, E. H. *Appl. Phys. Lett.* **2008**, *92*, 151115.
(9) (a) Taylor, J.; Kippeny, T.; Rosenthal, S. J. *J. Cluster Sci.* **2001**, *12*, 571. (b) Owen, J. S.; Park, J.; Trudeau, P.-E.; Alivisatos, A. P. *J. Am. Chem. Soc.* **2008**, *130*, 12279. (c) Kopping, J. T.; Patten, T. E. *J. Am. Chem. Soc.* **2008**, *130*, 5689.
(10) (a) Kovalenko, M. V.; Bodnarchuk, M. I.; Zaumseil, J.; Lee, J. S.; Talapin, D. V. *J. Am. Chem. Soc.* **2010**, *132*, 10085. (b) Kovalenko, M. V.; Scheele, M.; Talapin, D. V. *Science* **2009**, *324*, 1417. (c) Lee, J.-S.;

Kovalenko, M. V.; Huang, J.; Chung, D. S.; Talapin, D. V. *Nature Nanotechnol.* **2011**, *6*, 348.

(11) Dong, A.; Ye, X.; Chen, J.; Kang, Y.; Gordon, T.; Kikkawa, J. M.; Murray, C. B. *J. Am. Chem. Soc.* **2011**, *133*, 998.

(12) (a) Nag, A.; Kovalenko, M. V.; Lee, J.-S.; Liu, W.; Spokoyny, B.; Talapin, D. V. *J. Am. Chem. Soc.* **2011**, *133*, 10612. (b) Wills, A. W.; Kang, M. S.; Khare, A.; Gladfelter, W. L.; Norris, D. J. *ACS Nano* **2010**, *4*, 4523.

(13) Qu, L.; Peng, A.; Peng, X. *Nano Lett.* **2001**, *1*, 333.

(14) (a) Wang, F.; Tang, R.; Kao, J. L.-F.; Dingman, S. D.; Buhro, W. E. *J. Am. Chem. Soc.* **2009**, *131*, 4983. (b) Wang, F.; Tang, R.; Buhro, W. E. *Nano Lett.* **2008**, *8*, 3521.

(15) Jasieniak, J.; Smith, L.; van Embden, J.; Mulvaney, P.; Califano, M. *J. Phys. Chem. C* **2009**, *113*, 19468.

(16) (a) Marcus, Y. *The Properties of Solvents*; John Wiley and Sons: Chichester, 1999. (b) Godfrey, N. B. *Chem. Technol.* **1972**, *2*, 359.

(17) Jia, W.; McLachlan, J.; Xu, J.; Eichhorn, S. H. *J. Therm. Anal. Calorim.* **2010**, *100*, 839.

(18) Leatherdale, C. A.; Bawendi, M. G. *Phys. Rev. B* **2001**, *63*, 165315.

(19) Morris-Cohen, A. J.; Donakowski, M. D.; Knowles, K. E.; Weiss, E. A. *J. Phys. Chem. C* **2010**, *114*, 897.

(20) Gomes, R.; Hassinen, A.; Szczygiel, A.; Zhao, Q.; Vantomme, A.; Martins, J. C.; Hens, Z. *J. Phys. Chem. Lett.* **2011**, *2*, 145.

(21) (a) Nairn, J. J.; Shapiro, P. J.; Twamley, B.; Pounds, T.; von Wandruszka, R.; Fletcher, T. R.; Williams, M.; Wang, C.; Norton, M. G. *Nano Lett.* **2006**, *6*, 1218. (b) Purdy, A. P.; Berry, A. D.; George, C. F. *Inorg. Chem.* **1997**, *36*, 3370.

(22) Schapotschnikow, P.; Hommersom, B.; Vlugt, T. J. H. *J. Phys. Chem. C* **2009**, *113*, 12690.

(23) Fritzinger, B.; Capek, R. K.; Lambert, K.; Martins, J. C.; Hens, Z. *J. Am. Chem. Soc.* **2010**, *132*, 10195.

(24) Pickett, N. L.; Lawson, S.; Thomas, W. G.; Riddell, F. G.; Foster, D. F.; Cole-Hamilton, D. J.; Fryer, J. R. *J. Mater. Chem.* **1998**, *8*, 2769.

(25) (a) Danehy, J. P.; Parameswaran, K. N. *J. Chem. Eng. Data* **1968**, *13*, 386. (b) Freedman, L. D.; Doak, G. O. *Chem. Rev.* **1957**, *57*, 479.

(26) (a) Scragg, J. J.; Dale, P. J.; Peter, L. M.; Zoppi, G.; Forbes, I. *Phys. Stat. Sol. B* **2008**, *245*, 1772. (b) Riha, S. C.; Fredrick, S. J.; Sambur, J. B.; Liu, Y.; Prieto, A. L.; Parkinson, B. A. *ACS Appl. Mater. Interfaces* **2011**, *3*, 58. (c) Ye, H.; Park, H. S.; Akhavan, V. A.; Goodfellow, B. W.; Panthani, M, G.; Korgel, B. A.; Bard, A. J. *J. Phys. Chem. C* **2011**, *115*, 234.

(27) Brown, P.; Kamat, P. V. *J. Am. Chem. Soc.* **2008**, *130*, 8890.

(28) (a) Ellis, A. B.; Kaiser, S. W.; Wrighton, M. S *J. Am. Chem. Soc.* **1976**, *98*, 6855. (b) Natan, M. J.; Thackeray, J. W.; Wrighton, M. S. *J. Phys. Chem.* **1986**, *90*, 4089.